

FIRA
World Congress
Austria 2003

- **Preface** -
- **Topics** -
- **Committee** -
- **Program** -
- **List of Papers** -
- **Authors Index** -
- **Sessions** -
- **Instructions** -



Committee

General Chair

- ☛ P. Kopacek (Austria)

International Program Committee

- ☛ P. Albertos (Spain)
- ☛ H. S. Cho (Korea)
- ☛ R. Dillmann (Germany)
- ☛ T. Dinibütün (Turkey)
- ☛ G. Fürnsinn (Austria)
- ☛ F. Harashima (Japan)
- ☛ B. R. Hong (China)
- ☛ J. H. Kim (Korea)
- ☛ W. H. Kwon (Korea)
- ☛ D. Matko (Slovenia)
- ☛ J. Paiuk (Argentina)
- ☛ C. E. Pereira (Brazil)
- ☛ B. Reusch (Germany)
- ☛ N. Rozsenich (Austria)
- ☛ P. Robinson (UK)
- ☛ I. Rudas (Hungary)
- ☛ G. Schmidt (Germany)
- ☛ R. D. Schraft (Germany)
- ☛ J. Sitte (Australia)

National Organizing Committee

- ☛ M. W. Han (Chair)
- ☛ I. Nemetz
- ☛ B. Putz
- ☛ E. Schierer
- ☛ M. Würzl

Organized by

- ☛ Institute for Handling Devices and Robotics (IHRT),
Vienna University of Technology (VUT)
- ☛ Austrian Society for Automation and Robotics (ÖGART)
- ☛ Austrian Society for Measurement and Automation (ÖGMA)
- ☛ Austrian IFAC Supervisory Board



FIRA Robot World Congress 2003

October 1 - 3, 2003

Vienna Exhibition Centre, Austria



Prof. Ivan Petrovic
University of Zagreb
Faculty of Electrical Engineering and Computing
Unska 3
10000 Zagreb
Croatia

Re: *FIRA World Congress 2003*

Vienna, July 18, 2003

Dear Prof. Petrovi? !

The International Program Committee is pleased to inform you that your paper identified below has been accepted for presentation at the FIRA Robot World Congress 2003, October 1 - 3, 2003, Vienna Austria. To appear in the preprints of the Congress we must have the final version of your full paper specially typed (camera-ready copy) in electronic form (in PDF, PS and MS-Word) and in our hands by **August 15, 2003**.

You can download the detailed instructions for this shortly from the Webpage (<http://www.ihrt.tuwien.ac.at/FIRAWC03>).

Congratulations on the acceptance of your paper. We look forward to your successful participation in the FIRA Robot World Congress 2003 Vienna.

Ref.-No. : FIRA_055
Paper Title : Improvements of Occupancy Grid Maps by Sonar Data Corrections
Author (s) : Petrovi? Ivan Edouard Ivanjko
Comments :

Sincerely yours,

Prof. Peter Kopacek
(General Chair)

The congress organized by the

**Institute for Handling
Devices and Robotics,
Vienna University of Technology,
Austria**

General Chair
P. Kopacek (A)

Chairman
National Organizing Committee:
M.-W. Han (A)

Address for correspondence:

**FIRA Robot World Congress
2003**
Institute for Handling
Devices and Robotics (E318)
Vienna University of Technology,
Favoritenstraße 9-11
A-1040 Vienna

Phone: +43-1-58801 31801
Fax: +43-1-58801 31899
E-mail: fira03@ihrt.tuwien.ac.at

Improvements of Occupancy Grid Maps by Sonar Data Corrections

Edouard Ivanjko, Ivan Petrović, and Kristijan Maček
Department of Control and Computer Engineering in Automation,
Faculty of Electrical Engineering and Computing,
University of Zagreb,
HR-10000 Zagreb, Croatia
{edouard.ivanjko,ivan.petrovic,kristijan.macek}@fer.hr

Abstract

In this paper we address one of the major problems of mobile robots navigation, the creation of a map from local sensor data collected as the robot moves around an unknown environment. Map building is the problem of generating models of robot environments from sensor data and can be often referred as a concurrent mapping and localization problem. That is to build a consistent map, the mobile robot has to know its pose. We present here three approaches to create occupancy grid maps from sonar's data and suggest a simple solution to improve the mapping quality in cases of irregular disposition of the sonars. The proposed solution has been tested on the mobile robot Pioneer 2DX.

1 Introduction

Robotic mapping has been a highly active research area in robotics and artificial intelligence for past two decades. It addresses the problem of acquiring/generating spatial models of physical environments through mobile robots collecting local sensor data. The sensors that are mostly used are sonars, laser range finders and/or cameras [1]. The mapping problem contains also a localization problem. If the mobile robot doesn't know its location, it can't navigate effectively and achieve goals. In this paper the localization problem is solved using dead reckoning improved by a Kalman Filter [2]. Many types of the maps can be used for the robot navigation and localization. Maps can be based on topological (connection) or metric (distance) information, or a combination of the two [3]. Metric maps can be further refined by whether they use features or rely on dense surface information that doesn't distinguish features. The later approach has been applied in this paper. Namely, we have used occupancy grid maps, which

have become the dominant paradigm for environment modeling in mobile robotics [4]. An occupancy grid map presents a spatial representation of robot environment using a fine-grained, metric grid of variables that reflect the occupancy of the environments. Once acquired, it facilitates various key aspects of mobile robot navigation, such as localization, path planning and collision avoidance [1, 5, 6].

2 Robot Model

Mobile robot used in our experiments is a three-wheeled robot. Two front wheels are drive wheels with encoder mounted on them and the third wheel is a castor wheel needed for robot stability. Drive wheels can be controlled independently from each other. The kinematics of the mobile robot are given by the following relations (Figure 1):

$$x(k+1) = x(k) + v_t(k) \cdot T \cdot \cos \Theta(k+1), \quad (1)$$

$$y(k+1) = y(k) + v_t(k) \cdot T \cdot \sin \Theta(k+1), \quad (2)$$

$$\Theta(k+1) = \Theta(k) + \omega(k) \cdot T, \quad (3)$$

$$v_t(k) = \frac{v_L(k) + v_R(k)}{2} = \frac{\omega_L(k)R + \omega_R(k)R}{2}, \quad (4)$$

$$\omega(k) = \frac{v_R(k) - v_L(k)}{b} = \frac{\omega_R(k)R - \omega_L(k)R}{b}, \quad (5)$$

where are: $x(k)$ and $y(k)$ coordinates of the center of axle [mm]; $v_t(k)$ robot translation speed [mm/s]; T sampling time [s]; $\Theta(k)$ angle between the vehicle and x-axis [°]; $v_L(k)$ and $v_R(k)$ velocities of the left and right wheel, respectively [mm/s]; $\omega_L(k)$ and $\omega_R(k)$ angular velocities of the left and right wheel, respectively [rad/s]; R radius of the two wheels [mm], and b vehicle axle length [mm]. It is assumed that both wheels have equal radius. In order to compensate the systematic error regarding the unacquaintance of the exact wheel

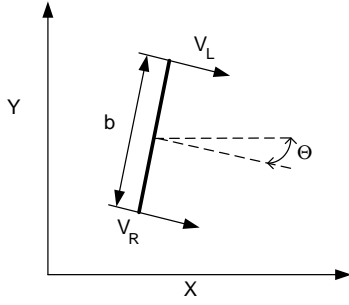


Figure 1: The Mobile Robot Kinematics.

radius and the unacquaintance of the exact axle length we expand the equations 4 and 5 with three additional parameters:

$$v_t(k) = \frac{k_1 \cdot v_L(k) + k_2 \cdot v_R(k)}{2}, \quad (6)$$

$$\omega(k) = \frac{k_2 \cdot v_R(k) - k_1 \cdot v_L(k)}{k_3 \cdot b}, \quad (7)$$

where parameters k_1 and k_2 compensate the unacquaintance of the exact wheel radius and parameter k_3 the unacquaintance of the exact axle length. Detailed explanation of used systematic error compensation and parameter value determination can be found in [7].

3 Dead-reckoning improvement by the Kalman Filter

Kalman filtering is a well-known technique for state and parameter estimations [8]. It is a recursive procedure that uses sequential sets of measurement. Prior knowledge of the state is expressed by the covariance matrix and it is improved at each step by taking prior estimates and new data for the subsequent state estimation. Using the Kalman Filter for localization [9] and mapping [3] is a common practice in mobile robotics. In our approach here the measurement vector used in localization is composed of the two translational speeds of left and right wheels and the mobile robot orientation measured by a compass (added to improve the orientation estimate in the x-y plane) [2]. These values are then used as input values for above described mobile robot kinematics model. The state estimate is denoted by $\hat{\mathbf{x}}$, \mathbf{z} is the measurement vector, \mathbf{r} is the residual vector and $\hat{\mathbf{z}}$ is the mea-

surement estimate:

$$\hat{\mathbf{z}} = \hat{\mathbf{x}} = \begin{bmatrix} \hat{v}_L & \hat{v}_R & \hat{\Theta} \end{bmatrix}^T, \quad (8)$$

$$\mathbf{z} = \begin{bmatrix} v_L & v_R & \Theta_c \end{bmatrix}^T, \mathbf{r} = \mathbf{z} - \hat{\mathbf{z}}.$$

Kalman Filter consists of two different steps: **propagation** and **update**. The equations for the propagation step are:

$$\hat{\mathbf{x}}_{k+1/k} = \Phi \cdot \hat{\mathbf{x}}_{k/k}, \quad (9)$$

$$P_{k+1/k} = \Phi \cdot P_{k/k} \cdot \Phi^T + Q. \quad (10)$$

The equations for the update step are:

$$K = P_{k+1/k} (P_{k+1/k} + R)^{-1}, \quad (11)$$

$$\hat{\mathbf{x}}_{k+1/k+1} = \hat{\mathbf{x}}_{k+1/k} + K \cdot \mathbf{r}, \quad (12)$$

$$P_{k+1/k+1} = (I - K)P_{k+1/k}. \quad (13)$$

In the above equations Φ is the system matrix, P is the error covariance matrix, Q is the system noise covariance matrix, K is the Kalman gain matrix and R is the measurement noise covariance matrix. Satisfying the above given robot model and applying the results from calibration discussed earlier, the system matrix Φ is given by:

$$\Phi = \begin{bmatrix} k_1 & 0 & 0 \\ 0 & k_2 & 0 \\ -\frac{T \cdot k_1}{k_3 \cdot b} \cdot \frac{180}{\pi} & \frac{T \cdot k_2}{k_3 \cdot b} \cdot \frac{180}{\pi} & 1 \end{bmatrix}. \quad (14)$$

4 Map Building

As mentioned above we are using occupancy grid maps. In mobile robotics, an occupancy grid is a two-dimensional tessellation of the environment into a grid G where each cell C_{ij} holds a part of environmental information [10]. The information can be of probabilistic or evidential character and is gathered with sensors (in our case sonars) mounted on the mobile robot. In most cases an occupancy grid is created by a robot exploring the environment, updating the grid recursively while moving. Often the updated cell information is just a number that represents the belief that this part of the environment is occupied by an object or free. We tested three strategies of building an occupancy grid map. The Bayesian approach, the Dempster-Shafer theory of evidence and Fuzzy set theory. The sonar sensor models used for these approaches are described in [4, 10].

4.1 The Bayesian Grid Map

The Bayesian approach of building an occupancy grid G relies on Bayes rule:

$$P(A_i | B) = \frac{P(A_i \cap B)}{P(B)}. \quad (15)$$

For a grid map building purpose the event A_i plays the role of a cell being occupied or not. Each cell C_{ij} of the grid map G is therefore associated with a binary random variable S_{ij} with states (O)cupied or (E)mpty for which:

$$P(S_{ij} = O) + P(S_{ij} = E) = 1. \quad (16)$$

Each cell C_{ij} in the Bayesian grid map has a state probability p_{ij} associated and is initialized as follows (usually the state probability value of 0.5 means that the cell occupancy value is unknown, for values bigger than 0.5 the cell is occupied, and for values smaller than 0.5 the cell is empty):

$$p_{ij} := 0.5 \quad \forall C_{ij} \in G. \quad (17)$$

When the Bayes grid map is updated using new sensor measurements, for each cell C_{ij} , which lies within the main lobe of the sensor, reading R the state probability value p_{ij} is updated according to:

$$p_{ij} := \frac{P(R|S_{ij}=O)p_{ij}}{P(R|S_{ij}=O)p_{ij} + [1 - P(R|S_{ij}=0)][1 - p_{ij}]}, \quad (18)$$

where $P(R|S_{ij} = O)$ represents the sensor model [4, 10]. Using this representation the same approach can be used with different sensors.

4.2 Dempster-Shafer Grid Map

In the Dempster-Shafer theory of evidence, a frame of discernment (FOD), denoted Θ is defined to be a finite set of mutually exclusive and exhaustive propositions. In the grid map case, each cell C_{ij} in the grid map G is characterized by two states (E)mpty or (O)cupied, and hence the FOD of grid cell C_{ij} is given by:

$$\Theta_{ij} = \{E, O\}. \quad (19)$$

Furthermore the Dempster-Shafer theory relies on a basic probability assignment (bpa) function:

$$m_{ij}^G : 2^{\Theta_{ij}} \rightarrow [0, 1], \quad (20)$$

where $2^{\Theta_{ij}}$ is the power set of Θ_{ij} , or in our case:

$$2^{\Theta_{ij}} = \{0, E, O, \{E, O\}\}. \quad (21)$$

The Dempster-Shafer grid map is initialized as follows:

$$m_{ij}^G(O) := 0, \quad m_{ij}^G(E) := 0, \quad m_{ij}^G(\{O, E\}) := 1 \quad \forall C_{ij} \in G. \quad (22)$$

When the Dempster-Shafer grid map is updated using new sensor measurements, for each cell C_{ij} which lies within the main lobe of the sensor reading R the bpa function values $m_{ij}^G(O)$ and $m_{ij}^G(E)$ are updated according to:

$$m_{ij}^G(O) := \frac{m_{ij}^G(O)m_{ij}^R(O) + m_{ij}^G(O)m_{ij}^R(\{O, E\}) + m_{ij}^G(\{O, E\})m_{ij}^R(O)}{1 - m_{ij}^G(E)m_{ij}^R(O) - m_{ij}^G(O)m_{ij}^R(E)} \quad (23)$$

$$m_{ij}^G(E) := \frac{m_{ij}^G(E)m_{ij}^R(E) + m_{ij}^G(E)m_{ij}^R(\{O, E\}) + m_{ij}^G(\{O, E\})m_{ij}^R(E)}{1 - m_{ij}^G(E)m_{ij}^R(O) - m_{ij}^G(O)m_{ij}^R(E)} \quad (24)$$

where $m_{ij}^R(O)$ and $m_{ij}^R(E)$ represent the sensor model [10]. Since this type of map stores two values for a cell (evidence that a cell is being occupied and evidence that a cell is being empty) the memory consumption and computation cost is doubled compared to the Bayesian map approach.

4.3 Fuzzy Grid Map

When applying fuzzy set theory to grid map building, two fuzzy sets (O)cupied and (E)mpty are defined. The defined fuzzy sets are complementary, i.e. for a given grid cell C_{ij} , partial membership to O and E is possible. The degree, with which the grid cells belong to E and O , is measured by two membership functions:

$$\mu_O^G : G \rightarrow [0, 1], \quad \mu_E^G : G \rightarrow [0, 1]. \quad (25)$$

The Fuzzy grid map is initialized with no membership to O and E :

$$\mu_O^G(C_{ij}) := 0, \quad \mu_E^G(C_{ij}) := 0, \quad \forall C_{ij} \in G. \quad (26)$$

When the Fuzzy grid map is updated using new sensor measurements, for each cell C_{ij} which lies within the main lobe of the sensor reading O the membership functions $\mu_O^G(C_{ij})$ and $\mu_E^G(C_{ij})$ are updated using the following algebraic sums:

$$\mu_O^G(C_{ij}) := \mu_O^G(C_{ij}) + \mu_O^R(C_{ij}) - \mu_O^G(C_{ij})\mu_O^R(C_{ij}) \quad (27)$$

$$\mu_E^G(C_{ij}) := \mu_E^G(C_{ij}) + \mu_E^R(C_{ij}) - \mu_E^G(C_{ij})\mu_E^R(C_{ij}) \quad (28)$$

where $\mu_O^R(C_{ij})$ and $\mu_E^R(C_{ij})$ represent the appropriate sensor models [10]. To track safe areas for the mobile robot to operate in a refined fuzzy set S is formed.

The membership function $\mu_S^G(C_{ij})$ of the safe fuzzy set is defined as:

$$\mu_S^G(C_{ij}) = (\mu_S^G(C_{ij}))^2 [1 - \mu_O^G(C_{ij})] \mu_C^G(C_{ij}), \quad \forall C_{ij} \in G, \quad (29)$$

with $\mu_C^G(C_{ij})$ defined as:

$$\mu_C^G(C_{ij}) = [1 - \mu_E^G(C_{ij})\mu_O^G(C_{ij})] [1 - (1 - \mu_E^G(C_{ij})) (1 - \mu_O^G(C_{ij}))]. \quad (30)$$

This type of map requires two values per cell, and with the computation of the safe fuzzy set S one more value is needed. This makes this type of map for one degree more computational and memory consuming than the Dempster-Shafer map.

5 Sonar Data Corrections

Mobile robots with cylindrical shape have usually regular angular distribution of the sonars on its body. However, mobile robots with more complex shapes often have irregular distribution of the sonars, which can cause some problems in map building based on sonar data. We have been using the Pioneer 2DX mobile robot from ActivMedia Robotics, which has 16 sonars grouped in four groups (Figure 2): i) six front sonars, ii) two left side sonars, iii) six rear sonars and iv) two right side sonars. Thus, there are areas of about 40 degrees angular space without any sonars. This results in a very bad environment representation in a local occupancy grid map. Figure 3 presents a local occupancy map when the mobile robot was placed in the leftmost position of a corridor (Figure 4). The light areas in the Figure 3 present empty space, dark areas present occupied space and gray areas unknown space. The local occupancy map should present walls on three sides and a open space in the front of the mobile robot. To compensate the bad sonar disposi-



Figure 2: Pioneer 2DX Mobile Robot.

tion a bounding box has been created using readings



Figure 3: Local occupancy map when robot is in the leftmost position of the corridor given in Figure 4.

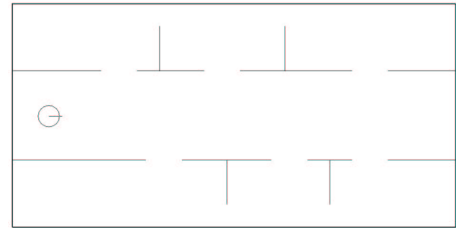


Figure 4: World model for the mapping experiments.

of the sonars that are perpendicular to the appropriate walls. This means that two front sonars have been used for the creation of the front side of the bounding box, two left side sonars for the creation of the left side of the bounding box and so on. The creation of a bounding box is illustrated in Figure 5. The circle in the middle is the mobile robot, the beams present the sonar main lobes and the rectangle around the mobile robot the created bounding box. The bad sonar disposition can be easily observed. At the front and rear sides of the robot there are no problems, but at the lateral sides there are insufficient data to ensure a good mapping quality. Readings of the sonars, which are not used for bounding box creation, are then modified to be in the bounding box. Modified values are marked by a black dot. Thus, measured ranges that fall outside the bounding box are modified to be on the bounding box border. It can be noticed that the modified value is the minimum value between the measured range and the bounding box modification. Using the proposed bounding box modification, local occupancy map obtained under equal condition as the map given in Figure 3 is shown in Figure 6. It can be seen that the local occupancy map now much better presents the surrounding walls and the open space in the front. The presented local occupancy maps are generated using the Bayesian approach. The same results were achieved with the other two mapping methods.

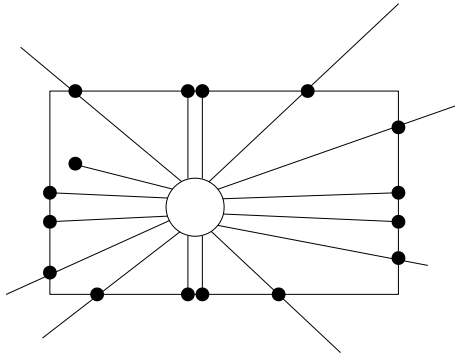


Figure 5: Bounding box creation.



Figure 6: Local occupancy map when robot is in the leftmost position of the corridor given in Figure 4 and when bounding box modification is applied.

6 Results

The described localization and mapping methods have been tested using the Pioneer 2DX mobile robot. The world model used for the experiments is shown in Figure 4. For each approach two separate experiments were made. One without the bounding box modification and one using the bounding box modification. In the first one sonar range readings greater than 3000 [mm] were rejected. This leads to the rejection of many sonar readings. The achieved results are presented in the Figures 7 to 12. Comparing the obtained results it can be seen that the bounding box modification improves the mapping, especially regarding the corridor corner areas. The bad side-effect is that the openings recognition is deteriorated. This negative effect isn't so expressive in the Bayes approach. In this case we achieved the best improvement. The side-effect is probably caused by the fact that bounding box has been created from the local data only. Therefore, past sonar readings have to be taken into consideration too. Certain distortion of all maps can be noticed in the Figures 7-12. This is because algorithms for robot

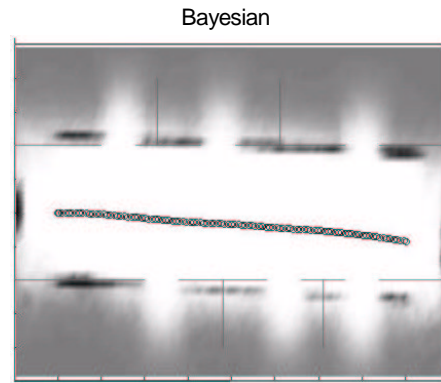


Figure 7: Corridor map using the Bayes approach.

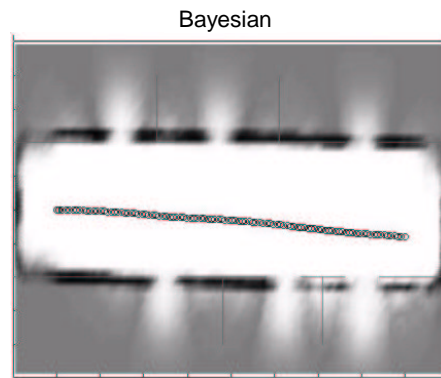


Figure 8: Corridor map using Bayes approach and the bounding box modification.

tracking have not been yet implemented.

7 Conclusion and Future Work

We address the problem of on-line occupancy grid map building based on sonar data. Particular attention is paid to the problems caused by irregular disposition of the sonars on the robot body. A simple effective solution, based on bounding box creation, has been found for the alleviation of these problems. The solution was tested on the mobile robot Pioneer 2DX. Considerable improvements have been achieved in the Bayes and Dempster-Shafer mapping approaches. A negative side-effect regarding the opening detection deterioration was observed. In order to reduce this side-effect we plan to include past sonar readings in the creation of the bounding box. To improve the localization we plan to implement an Extended Kalman Filter for fusion of dead-reckoning and sonar data.

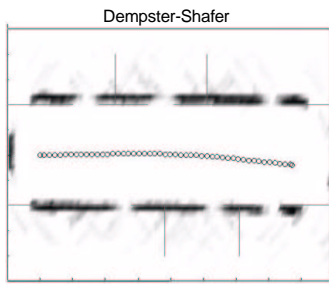


Figure 9: Corridor map using the Dempster-Shafer approach.

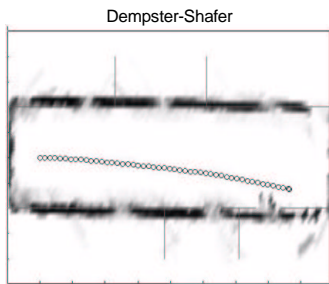


Figure 10: Corridor map using Dempster-Shafer approach and the bounding box modification.

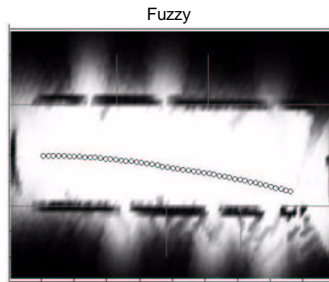


Figure 11: Corridor map using the Fuzzy approach.

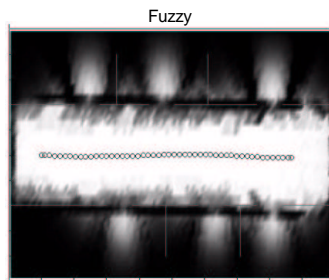


Figure 12: Corridor map using Fuzzy approach and the bounding box modification.

References

- [1] Wolfram Burgard, Armin B. Cremers, Dieter Fox, Dirk Hähnel, Gerhard Lakemeyer, Dirk Schulz, Walter Steiner, Sebastian Thrun, Experiences with an interactive museum tour-guide robot, *Artificial Intelligence (AI)*, 114(1-2), pp. 3-55, 1999.
- [2] Ivan Petrović, Edouard Ivanjko, Nedjeljko Perić, *Neural Network Based Correction of Odometry Errors in Mobile Robots*, Proceedings of FIRA Congress 2002, pp. 91-96, 2002.
- [3] Sebastian Thrun, *Robotic Mapping: A Survey*, Carnegie Mellon University, Technical Report CMU-CS-02-111, 2002.
- [4] Alberto Elfes, *Using Occupancy Grids for Mobile Robot Perception and Navigation*, Proceedings of IEEE International Conference on Robotics and Automation, Vol. 2, pp. 727-733, 1988.
- [5] Juan D. Tardós, José Neira, Paul M. Newman, John J. Leonard, Robust Mapping and Localization in Indoor Environments using Sonar Data, *To appear in the International Journal of Robotics Research*, Technical Memorandum 2001-04, 2001.
- [6] J. Borenstein, Y. Koren, The Vector Field Histogram - Fast Obstacle Avoidance for Mobile Robots, *IEEE Journal of Robotics and Automation*, Vol. 7, No 3, pp. 278-288, 1991.
- [7] Edouard Ivanjko, Ivan Petrović, Nedjeljko Perić, *An Approach to Odometry Calibration of Differential Drive Mobile Robots*, accepted on Electrical Drives and Power Electronics International Conference EDPE'03, 2003.
- [8] Greg Welch, Gary Bishop, An Introduction to the Kalman Filter, *University of North Carolina at Chapel Hill*, TR 95-041, 2000.
- [9] P. Goel, S.I. Roumeliotis, G.S. Sukhatme, *Robust Localization Using Relative and Absolute Position Estimates*, Proceedings of the IEEE/RSJ International Conference on Intelligent Robots and Systems (IROS), 1999.
- [10] Olle Wijk, *Triangulation Based Fusion of Sonar Data with Application in Mobile Robot Mapping and Localization*, Royal Institute of Technology (KTH) Sweden, PhD Thesis, 2001.

Acknowledgement

This research has been supported by the Ministry of Science and Technology of the Republic of Croatia under grant No. 0036018.